

An In Vitro Experimental Study of the Pulse Delivery Method in Irreversible Electroporation

Bing Zhang¹

Mem. ASME

Division of Biomedical Engineering,
University of Saskatchewan,
Saskatoon, SK S7N 5A2, Canada
e-mail: bing.zhang84@usask.ca

Michael A. J. Moser

Department of Surgery,
University of Saskatchewan,
Saskatoon, SK S7N 5A2, Canada
e-mail: mam305@mail.usask.ca

Edwin M. Zhang

Department of Medical Imaging,
Division of Vascular and Interventional Radiology,
University of Toronto,
Toronto, ON M5S, Canada
e-mail: edwinmzhang@gmail.com

Jim Xiang

Saskatchewan Cancer Agency,
University of Saskatchewan,
Saskatoon, SK S7N 5A2, Canada
e-mail: jim.xiang@usask.ca

Wenjun Zhang

Fellow ASME
Division of Biomedical Engineering,
University of Saskatchewan,
Saskatoon, SK S7N 5A2, Canada;
Department of Mechanical Engineering,
University of Saskatchewan,
Saskatoon, SK S7N 5A2, Canada
e-mail: chris.zhang@usask.ca

The purpose of this study was to investigate the feasibility of generating larger ablation volumes using the pulse delivery method in irreversible electroporation (IRE) using a potato model. Ten types of pulse timing schemes and two pulse repetition rates (1 pulse per 200 ms and 1 pulse per 550 ms) were proposed in the study. Twenty in vitro experiments with five samples each were performed to check the effects on the ablation volumes for the ten pulse timing schemes and two pulse repetition rates. At the two pulse repetition rates (1 pulse per 200 ms and 1 pulse per 550 ms), the largest ablation volumes achieved were $1634.1 \text{ mm}^3 \pm 122.6$ and $1828.4 \text{ mm}^3 \pm 160.9$, respectively. Compared with the baseline approach (no pulse delays), the ablation volume was increased approximately by 62.8% and 22.6% at the repetition rates of 1 pulse per 200 ms and 1 pulse per 550 ms, respectively, using the pulse timing approach (with pulse delays). With the pulse timing approach, the ablation volumes generated at the lower pulse repetition rate were significantly larger than

those generated at the higher pulse repetition rate ($P < 0.001$). For the experiments with one pulse train (baseline approach), the current was $5.2 \text{ A} \pm 0.4$. For the experiments with two pulse trains, the currents were $6.4 \text{ A} \pm 0.9$ and $6.8 \text{ A} \pm 0.9$, respectively ($P = 0.191$). For the experiments with three pulse trains, the currents were $6.6 \text{ A} \pm 0.6$, $6.9 \text{ A} \pm 0.6$, and $6.5 \text{ A} \pm 0.6$, respectively ($P = 0.216$). For the experiments with five pulse trains, the currents were $6.6 \text{ A} \pm 0.9$, $6.9 \text{ A} \pm 0.9$, $6.5 \text{ A} \pm 1.0$, $6.5 \text{ A} \pm 1.0$, and $5.7 \text{ A} \pm 1.2$, respectively ($P = 0.09$). This study concluded that: (1) compared with the baseline approach used clinically, the pulse timing approach is able to increase the volume of ablation; but, the pulse timing scheme with the best performance might be various with the tissue type; (2) the pulse timing approach is still effective in achieving larger ablation volumes when the pulse repetition rate changes; but, the best pulse timing scheme might be different with the pulse repetition rate; (3) the current in the baseline approach was significantly smaller than that in the pulse timing approach. [DOI: 10.1115/1.4038238]

Keywords: irreversible electroporation, large ablation zones, potato model, pulse repetition rate, pulse timing

Introduction

Irreversible electroporation (IRE) is a promising medical modality that uses high magnitude electric pulses (hundreds to thousands of V/cm) to dramatically increase permeability in tumor cell membranes [1]. The mechanism whereby IRE causes ablation is believed to be due to the creation of nanometer-size “pores” when the plasma membrane is exposed to the external pulsed electric field [2]. There have been several types of theoretical models explaining the formation of the pores in the cell membrane. The model proposed by Kinoshita et al. [3] has been considered as the one that is able to explain the process of electroporation comprehensively and sophisticatedly. This model believes that the formation of pores is due to the interaction between the trans-membrane voltage (potential drop across the membrane in the external electric field) and the cell membrane with its intrinsic physical properties, such as line tension and surface tension. For the situation in which the cells can recover after the external electric field is removed, the process is called reversible electroporation otherwise IRE. In the case of IRE, permanent membrane lysis, consumption of adenosine triphosphate, and eventual loss of homeostasis (i.e., loss of cellular contents) are considered as factors that lead to the cell death [1].

As a monotherapy (i.e., no cytotoxic drugs, not in conjunction with thermal effects) to destroy tumor cells, first proposed by Davalos et al. a decade ago [4], IRE has received widespread interest from the scientific community and become a burgeoning modality in clinical practice for the ablation of various tumors in different organs, such as liver, pancreas, kidney, lung, lymph node, and pelvis [5]. Compared with other tumor ablation modalities, especially thermal-based modalities [6–9], IRE has two important advantages: (1) no collateral thermal effect, making it safe in anatomically sensitive areas such as near major blood vessels or the bowel, and (2) absence of heat sink effect which limits the effectiveness of thermal ablation methods near large blood vessels. However, some issues of IRE need to be addressed to improve it to be a favorable treatment in clinic, such as: (1) no systematic way to determine the threshold of the electric field, which varies depending on the type of tumors, and the threshold is coupled with other IRE operation parameters such as pulse duration, pulse number, pulse repetition rate, pulse strength, and electrode exposure length, and (2) inability to easily destroy large (>3 or 4 cm) size tumors.

Studies have been performed to address the aforementioned two issues in literature. For issue (2), Jiang et al. [10,11] proposed a new approach called “pulse timing” based on the prostate tumor cell lines. Differing from the usual way of pulse delivery (pulses delivered as an integral train, commonly referred to as the

¹Corresponding author.

Manuscript received July 16, 2017; final manuscript received September 27, 2017; published online November 7, 2017. Assoc. Editor: Osama Mukdadi.

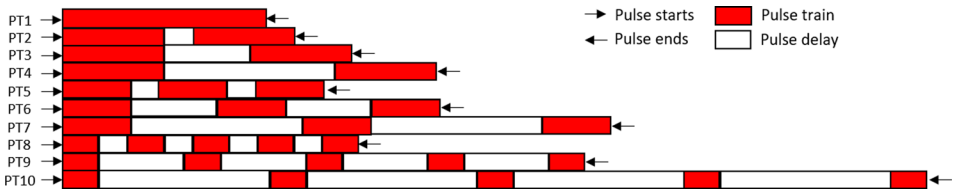


Fig. 1 Diagram of ten pulse timing schemes proposed in the study

Table 1 The in vitro experiment proposed in the study

Experiment #	N	Pulse duration (μ s)	Pulse strength (V)	Pulse repetition rate	Number of pulses (pulse timing)
1	5	90	1000	1 pulse per 200 ms	90
2					90 (2 \times 45 with 10 s delays)
3					90 (2 \times 45 with 30 s delays)
4					90 (2 \times 45 with 60 s delays)
5					90 (3 \times 30 with 10 s delays)
6					90 (3 \times 30 with 30 s delays)
7					90 (3 \times 30 with 60 s delays)
8					90 (5 \times 18 with 10 s delays)
9					90 (5 \times 18 with 30 s delays)
10					90 (5 \times 18 with 60 s delays)
11				1 pulse per 550 ms	90
12					90 (2 \times 45 with 10 s delays)
13					90 (2 \times 45 with 30 s delays)
14					90 (2 \times 45 with 60 s delays)
15					90 (3 \times 30 with 10 s delays)
16					90 (3 \times 30 with 30 s delays)
17					90 (3 \times 30 with 60 s delays)
18					90 (5 \times 18 with 10 s delays)
19					90 (5 \times 18 with 30 s delays)
20					90 (5 \times 18 with 60 s delays)

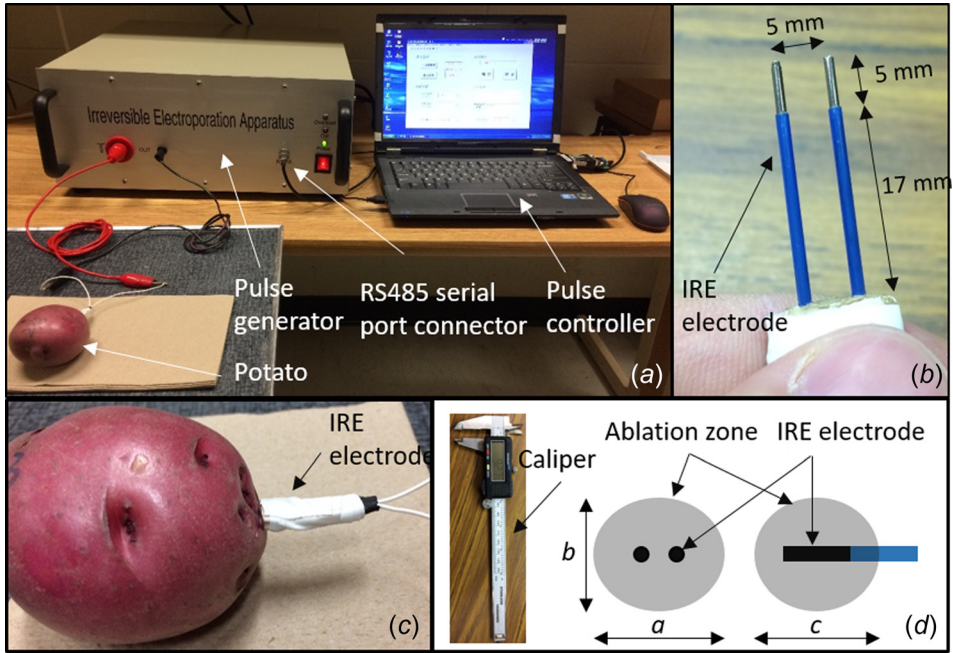


Fig. 2 Experimental setup for in vitro experiments proposed in the study: (a) experimental setup, (b) IRE electrode, (c) potato with IRE electrode insertion, and (d) ablation zone and caliper

baseline approach in the literature [11]), the pulse timing approach is based on the concept of pulse delay, i.e., pulses are delivered as several separate pulse trains with a time delay (no pulse is delivered during the delay time) between two pulse trains. They demonstrated that this method can inhibit the growth of localized prostate tumors in mice, which is further explained as more tumor destruction compared to the baseline approach [10,11]. They explained that the underlying mechanism for this result is relevant to the change to membrane properties and the increased pore recovery time [11]. This mechanism is not comprehensive and warrants further study. Besides, there are still some unanswered questions. The first question is whether the pulse timing approach is applicable to other types of tissues or whether the pulse timing approach is tissue-dependent. The second question is whether the pulse repetition rate may affect the effectiveness of the pulse timing approach.

The goal of this study was to provide answers to the aforementioned questions through an in vitro experiment. Particularly, the study examined the two factors, that is, the pulse timing scheme and the pulse repetition rate, on the ablation volume of IRE. The experiment was conducted on the potato model.

Materials and Methods

Pulse Delivery Method. Ten pulse timing schemes (PT1–PT10) with 90 pulses for each were used in the in vitro experiment, as shown in Fig. 1. For PT1, the 90 pulses were delivered in one train without any delay, which is one of the standard settings in clinical practice (called the baseline approach) [12,13]. For PT2, PT3, and PT4, the 90 pulses were delivered in two trains of 45 pulses with delays of 10 s, 30 s, and 60 s between the two trains, respectively. For PT5, PT6, and PT7, the 90 pulses were delivered in three trains of 30 pulses with delays of 10 s, 30 s, and 60 s between any two trains, respectively. For PT8, PT9, and PT10, the 90 pulses were delivered in five trains of 18 pulses with delays of 10 s, 30 s, and 60 s between any two trains, respectively.

Two types of repetition rates were used in the experiment: 1 pulse per 200 ms and 1 pulse per 550 ms. In the experiment, other parameters of IRE were set as constants (i.e., pulse duration of 90 μ s, and pulse strength of 1000 V) in light of the focus of the experiment on the pulse timing scheme and repetition rate. The pulse duration was determined from the clinically relevant setting [14], and the pulse strength was determined by several pretests. In these

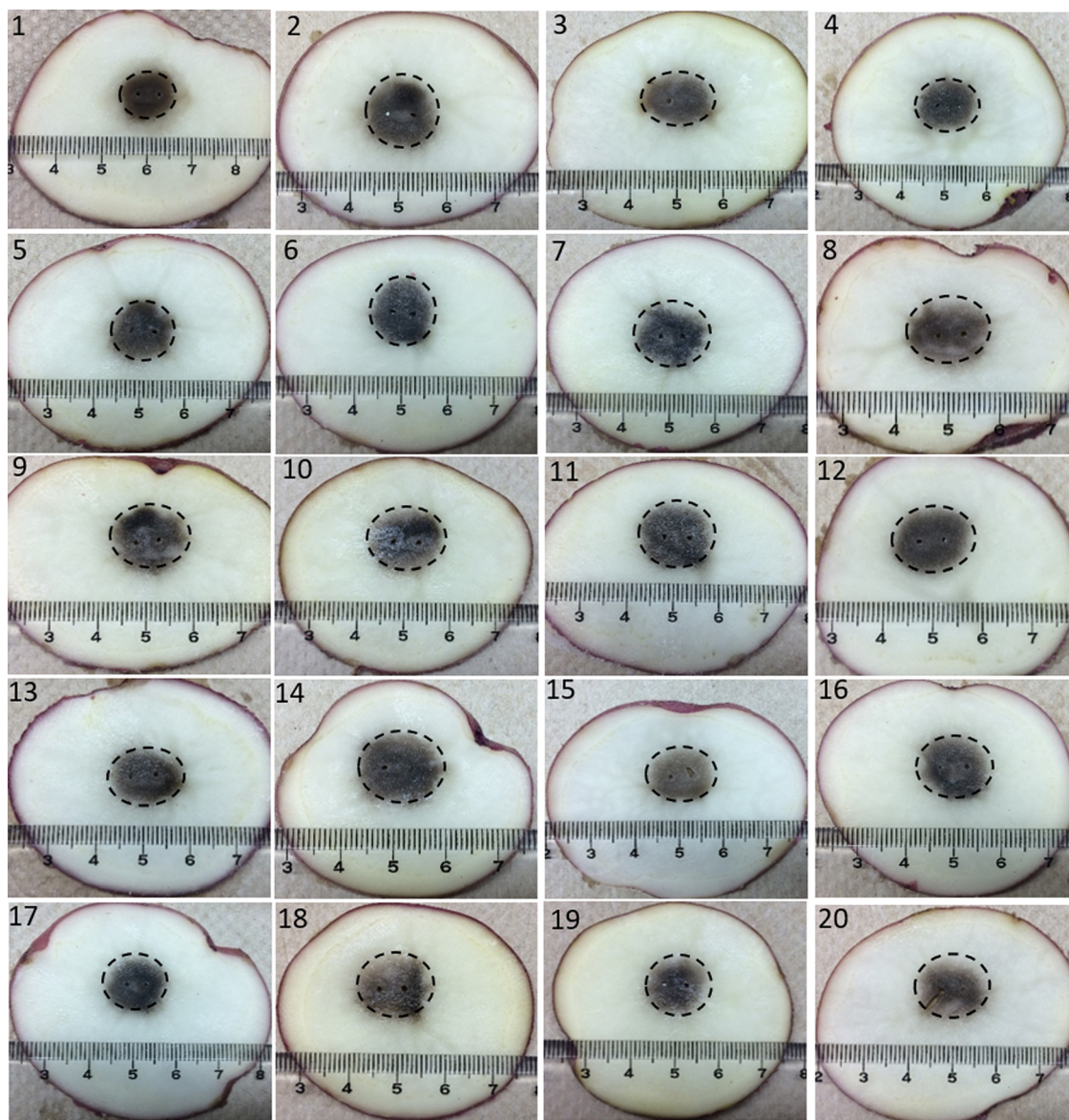


Fig. 3 Representative images of ablation zone of in vitro experiments (the number on each image means the experiment number)

tests, three pulse strengths (i.e., 500, 1000, and 1500 V) were tested. The pulse strength of 500 V was found not high enough to generate marked and measurable ablation zones after 24 h; and the pulse strength of 1500 V was found too high leading to crashes of the pulse generator (i.e., >50 A). So the pulse strength of 1000 V was used in the study. In total, there were 20 in vitro experiments, see Table 1 for details of these setups.

Experimental Setup. In this study, American potatoes (red) were selected as the model. It is noted that many previous studies showed that potatoes are a highly relevant and well-accepted model in the in vitro study of IRE due to its similar manner in responding to the electroporation as mammalian cells [15–18]. Therefore, the use of the potato model for the in vitro study is widely accepted, such as the design of new IRE electrode [15,17] and the improved pulse delivery method [19,20]. A custom-made electric pulse generator and a monopolar IRE electrode were used to perform the experiments (Fig. 2(a)). The pulse generator was able to deliver 0–3000 V of electric pulses in a rectangular wave shape with 90 μ s of pulse duration. The pulse delivery was controlled by the pulse controller (a computer system with a pulse control algorithm). The IRE apparatus was connected to the pulse controller with the RS485 serial port connector. The IRE electrode was designed with two electrodes (Ni–Ti alloy, one acting as anode and another being cathode) with 1 mm in diameter, 5 mm in length each, and 5 mm (center to center) in distance, as shown in Fig. 2(b).

In total, 100 potatoes (with the mean size of each potato being $70.7 \times 62.3 \times 52.1$ mm³) purchased from a local grocery store and divided into 20 groups randomly were conducted in this experiment, so for each experiment, there were five potatoes ($N = 5$ for each experiment in Table 1). The electrode was inserted into the potato model along the long axis of the potato with the insertion depth of 22 mm to avoid the boundary effects, as shown in Fig. 2(c). Orientation of the polarity was arranged between the cathode and anode electrode to alleviate oxidation effects resulting from delivering many experiments in the same cathode–anode orientation [21]. Each electrode was scraped clean with a blade on a regular basis to eliminate the layer of oxidation.

The treated potatoes were stored in paper plates at ambient temperature (i.e., 21 °C) for 24 h, after which ablation zones were identified by the darkened area (see Fig. 3) on the tissue. The ablation zones were sliced perpendicular to the IRE electrode at 1–2 mm intervals and then measured using the caliper (Fig. 2(d)). The volume of ablation zone was calculated using the formula for the volume of an ellipsoid, i.e.,

$$V_{\text{exp}} = (1/6)\pi abc \quad (1)$$

where a , b , and c are the width, height, and length, respectively, as shown in Fig. 2(d).

Statistical Analysis. Each experiment was performed in quintuplicate, and the result was given as mean \pm standard deviation. One-way ANOVA was employed to assess for a statistically significant difference in the results using MINITAB 17 (Minitab, Inc., State College, PA). Results were considered as statistically significant at $P < 0.05$.

Results and Discussion

Table 2 shows the dimensions of the ablation zone of each in vitro experiment under different pulse delivery methods using the potato model. The ablation volume was obtained by using Eq. (1). Figure 3 shows the representative results of ablation zone ($N = 5$) from the in vitro experiment. The slice with the largest dimensions of ablation zone (i.e., a and b as shown in Fig. 2(d)) of each experiment was used to take the image.

For different pulse repetition rates, the pulse timing approach is still able to increase the volume of ablation compared with the

baseline approach. As shown in Fig. 4(a), the largest ablation volume ($1634.1 \text{ mm}^3 \pm 122.6$, $P < 0.001$) was generated by using the pulse timing scheme of 90 pulses in two trains of 45 pulses with delay of 10 s (PT2) when the pulse repetition rate was 1 pulse per 200 ms. However, for the pulse repetition rate of 1 pulse per 550 ms, the largest ablation volume ($1828.4 \text{ mm}^3 \pm 160.9$, $P < 0.035$) was generated by using the pulse timing scheme of 90 pulses in two trains of 45 pulses with delay of 60 s (PT4), as shown in Fig. 4(b). Compared with the baseline approach, the ablation volume was increased approximately by 62.8% and 22.6% at the pulse repetition rates of 1 pulse 200 ms and 1 pulse per 550 ms, respectively. It is interesting to note that the period of delay time for the pulse delivery method with the lower repetition rate (i.e., 1 pulse per 550 ms) is longer than that for the pulse delivery method with the higher repetition rate (i.e., 1 pulse per 200 ms). The process of cell permeabilization and membrane resealing in tissues is highly relevant to the pulse duration, the pulse repetition rate, and the pulse delay time [1,22]. For different pulse repetition rates, the optimal setting of the pulse timing scheme for the cell permeabilization may be different. We believe that this phenomenon is also relevant to the type of tissue cell and worth studying further for increasing the volume of ablation for different cells during IRE application. Furthermore, the effectiveness of pulse timing approach is regardless of the pulse repetition rate. At both pulse repetition rates, there is a significant difference in the ablation volumes generated by different pulse timing schemes (i.e., PTs 2–10) ($P = 0.008$ and $P = 0.003$, respectively).

For the baseline approach (PT1), compared to the higher repetition rate (i.e., 1 pulse per 200 ms), the pulse delivery method with the lower repetition rate (i.e., 1 pulse per 550 ms), is more efficient in achieving a larger ablation volume ($1490.1 \text{ mm}^3 \pm 251.2$ versus $1003.8 \text{ mm}^3 \pm 196.5$, $P = 0.009$). This lower repetition rate is closer to the electrocardiogram-synchronized pulse delivery pattern commonly used in clinical settings, and this result is in accordance with the conclusion obtained by Silve et al. [23]. The same conclusion (lower repetition rate is more efficient than higher repetition rate) was also obtained for PT3 ($1136.8 \text{ mm}^3 \pm 60.9$ versus $1453.3 \text{ mm}^3 \pm 59.4$, $P < 0.001$) and PT4 ($1102.1 \text{ mm}^3 \pm 214.4$ versus $1828.4 \text{ mm}^3 \pm 160.9$, $P < 0.001$). These results also confirmed that the pulse timing approach is still effective when the pulse repetition rate is at about the electrocardiogram-synchronized rate. For the other pulse timing schemes (i.e., PT2 and PTs 5–10), however, there was no significant difference in the ablation volume between the two pulse repetition rates, as shown in Fig. 5.

Table 2 Dimensions of ablation zone of each in vitro experiments

Experiment #	a (mm)	b (mm)	c (mm)	V_{exp} (mm ³)
1	11.9 ± 1.1	11.2 ± 1.0	14.2 ± 0.4	1003.8 ± 196.5
2	14.5 ± 0.4	13.8 ± 0.2	15.6 ± 0.9	1634.1 ± 122.6
3	14.2 ± 0.9	11.2 ± 0.7	13.7 ± 0.2	1136.8 ± 60.9
4	13.3 ± 0.9	11.7 ± 0.9	13.5 ± 0.9	1102.1 ± 214.1
5	14.2 ± 0.1	14.5 ± 0.9	13.4 ± 1.1	1454.7 ± 186.0
6	13.1 ± 0.3	13.4 ± 1.3	13.8 ± 1.2	1278.2 ± 219.3
7	13.6 ± 1.8	12.6 ± 0.9	14.1 ± 0.9	1255.1 ± 171.7
8	14.0 ± 1.0	12.2 ± 1.0	15.0 ± 1.2	1340.2 ± 205.8
9	15.2 ± 0.8	13.5 ± 0.5	14.1 ± 0.9	1517.2 ± 210.4
10	14.4 ± 1.8	12.4 ± 2.8	13.2 ± 2.0	1295.5 ± 535.2
11	14.5 ± 0.8	13.2 ± 0.7	14.8 ± 1.1	1491.1 ± 251.2
12	14.7 ± 0.5	14.1 ± 0.1	14.2 ± 0.1	1542.9 ± 56.2
13	14.7 ± 0.4	14.1 ± 0.8	13.4 ± 0.1	1453.3 ± 59.4
14	15.6 ± 0.7	14.9 ± 0.7	15.0 ± 0.8	1828.4 ± 160.9
15	13.5 ± 1.6	12.8 ± 1.3	13.5 ± 1.2	1243.2 ± 312.9
16	14.6 ± 1.1	14.1 ± 0.9	13.9 ± 1.3	1496.0 ± 260.1
17	12.6 ± 1.0	11.6 ± 1.0	14.3 ± 0.8	1100.5 ± 211.0
18	15.5 ± 1.1	13.7 ± 0.7	13.9 ± 0.9	1544.8 ± 175.6
19	15.2 ± 0.8	13.8 ± 0.1	12.9 ± 0.8	1408.1 ± 94.5
20	15.2 ± 1.6	12.5 ± 1.5	13.3 ± 2.2	1421.2 ± 416.3

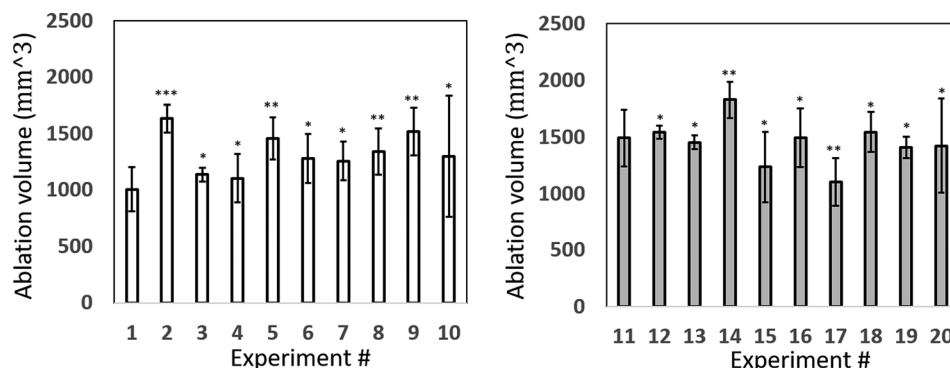


Fig. 4 Ablation volumes of in vitro experiments under the same pulse repetition rate: (a) 1 pulse per 200 ms and (b) 1 pulse per 550 ms (* $P > 0.05$, ** $P < 0.05$, and *** $P < 0.001$)

The currents varied by potato impedances and pulse delivery methods were shown in Table 3. For the experiments with one pulse train (baseline approach), the current was 5.2 ± 0.4 . For the experiments with two pulse trains, the currents were 6.4 ± 0.9 and 6.8 ± 0.9 , respectively ($P = 0.191$). For the experiments with three pulse trains, the currents were 6.6 ± 0.6 , 6.9 ± 0.6 , and 6.5 ± 0.6 , respectively ($P = 0.216$). For the experiments with five pulse trains, the currents were 6.6 ± 0.9 , 6.9 ± 0.9 , 6.5 ± 1.0 , 6.5 ± 1.0 , and 5.7 ± 1.2 , respectively ($P = 0.09$). No significant difference in the current between the pulse trains was found for all the experiments. However, it is interesting to note that the current in the experiments with one pulse train was significantly smaller than that in the experiments with multiple pulse trains ($P < 0.001$). However, the ablation volumes generated by pulse trains with higher current (experiments 2–10 and 12–20) were found to be similar with that generated by pulse trains with lower current (experiments 1 and 11) ($P = 0.136$). The reasons behind these phenomena are worth studying further, as it would be useful for avoiding the crash of a pulse generator when higher pulse strengths are applied for larger ablation volumes.

In this study, the temperature change was also investigated using a commercial temperature probe (HKMTSS-040 U-6, Omega, Laval, QC, Canada) for all the experiments. The

temperature probe was inserted into one of the insertion holes of IRE electrode to measure the temperature just after IRE application. No lethal temperatures (e.g., $>50^\circ\text{C}$) that can generate thermal damage to potato tissues were found. This is in agreement with the study of Ref. [24] using the animal models in which they concluded that for 90 pulses, lethal temperatures were generated only if the voltage was greater than 2500 V (versus 1000 V in this study).

Many studies have indicated that electroporation is a process that shows memory effects, which means that its behavior depends on previous pulse delivery history [16,25,26]. Thus, this phenomenon brings opportunities to increase the volume of ablation by optimizing the pulse delivery method for IRE applications. By using a potato model, this study investigated the effects on the ablation volume when varying IRE pulse delivery methods, specifically the pulse timing and pulse repetition rate. This study further confirms and expands on the potential utility of the pulse timing approach for increasing the volume of ablation by IRE. It is worth noting that, due to the different electric field thresholds for IRE between the potato and mammalian tissues, the ablation sizes created in this study may not be directly related to those expected clinically. A limitation of this study might be that the repetition rate of 1 Hz (commonly used in clinical settings) was

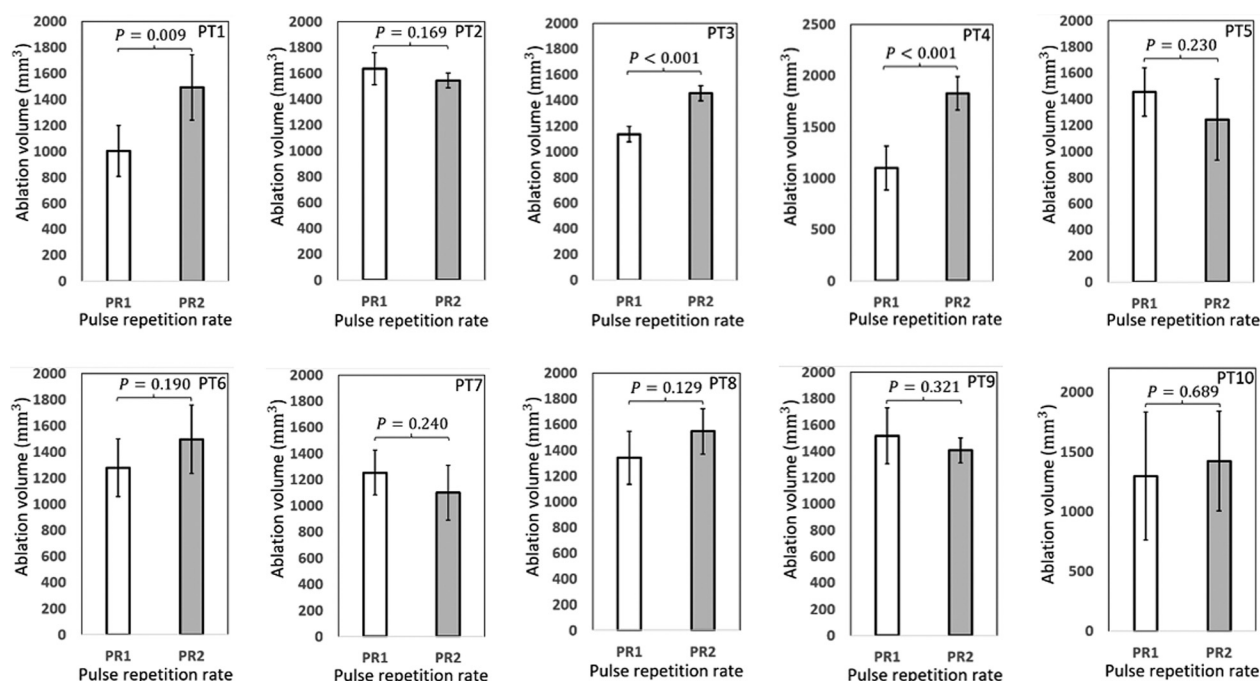


Fig. 5 Comparisons of ablation volumes of in vitro experiments under the same pulse timing scheme (PR1: 1 pulse per 200 ms and PR2: 1 pulse per 550 ms)

Table 3 Comparison of potato currents for IRE applications at 1000 V

Experiment #	First pulse train	Second pulse train	Third pulse train	Fourth pulse train	Fifth pulse train
1 and 11	5.2A \pm 0.4	—	—	—	—
2, 3, 4, 12, 13, and 14	6.4A \pm 0.9	6.8A \pm 0.9	—	—	—
5, 6, 7, 15, 16, and 17	6.6A \pm 0.6	6.9A \pm 0.6	6.5A \pm 0.6	—	—
8, 9, 10, 18, 19, and 20	6.6A \pm 0.9	6.9A \pm 0.9	6.5A \pm 1.0	6.5A \pm 1.0	5.7A \pm 1.2

not considered in the study due to the limitation of the custom pulse generator. To further verify and fully understand the pulse timing approach, future studies are warranted to investigate that: (1) whether the pulse strength affects the effectiveness of pulse timing approach to increase the ablation volume; (2) whether the effectiveness of pulse timing approach is stronger at higher pulse repetition rates.

Given that the size of ablation zone is determined to some extent by the electrode placement, limited by the fact that the electrodes cannot be more than 2.5 cm apart, the increase in ablation zone seen in our study by 25–60% is significant. Such an adjustment to the classic IRE ablation may allow for lower energy and heat to be used and still result in equal effectiveness or it may allow for the use of the same energy levels and an increased effectiveness. The margins of the ablation should be better ablated with this new approach, and this should translate to a lower risk of recurrence at the margins. The conclusion that the pulse delivery method (i.e., pulse timing and pulse repetition rate) plays a significant role in the increase of ablation volume during IRE treatment should be applied to various types of tissues; for different types of tissue cells, the optimal pulsing timing scheme for the largest ablation volume might be different. Such a statement is based on the results reported in the literature [10,11] and this study.

Conclusions

The conclusions that can be drawn from the present study are as follows:

- (1) Compared with the baseline approach in clinical practice, the pulse timing approach is able to increase the volume of ablation on the potato model; but, the pulse timing scheme with the best performance might be various with the tissue type.
- (2) The pulse timing approach is still effective in achieving larger ablation volumes when the pulse repetition rate changes; but, the best pulse timing scheme might be different with the pulse repetition rate.
- (3) The current in the baseline approach was significantly smaller than that in the pulse timing approach.

Funding Data

- Royal University Hospital Foundation (Saskatoon, SK, Canada) (Grant No. 1-417578).
- National Sciences and Engineering Research Council of Canada (NSERC).
- National Natural Science of China (Grant No. 51375166).

References

- [1] Jiang, C., Davalos, R. V., and Bischof, J. C., 2015, "A Review of Basic to Clinical Studies of Irreversible Electroporation Therapy," *IEEE Trans. Biomed. Eng.*, **62**(1), pp. 4–20.
- [2] Yarmush, M. L., Golberg, A., Serša, G., Kotnik, T., and Miklavčič, D., 2014, "Electroporation-Based Technologies for Medicine: Principles, Applications, and Challenges," *Annu. Rev. Biomed. Eng.*, **16**(1), pp. 295–320.
- [3] Kinoshita, K., Jr., Ashikawa, I., Saita, N., Yoshimura, H., Itoh, H., Nagayama, K., and Ikegami, A., 1988, "Electroporation of Cell Membrane Visualized Under a Pulsed-Laser Fluorescence Microscope," *Biophys. J.*, **53**(6), p. 1015.
- [4] Davalos, R. V., Mir, L., and Rubinsky, B., 2005, "Tissue Ablation With Irreversible Electroporation," *Ann. Biomed. Eng.*, **33**(2), pp. 223–231.
- [5] Scheffer, H. J., Nielsen, K., de Jong, M. C., van Tilborg, A. A., Vieveen, J. M., Bouwman, A. R., Meijer, S., van Kuijk, C., van den Tol, P. M., and Meijerink, M. R., 2014, "Irreversible Electroporation for Nonthermal Tumor Ablation in the Clinical Setting: A Systematic Review of Safety and Efficacy," *J. Vasc. Interv. Radiol.*, **25**(7), pp. 997–1011.
- [6] Zhang, B., Moser, M. A., Zhang, E. M., Luo, Y., Liu, C., and Zhang, W., 2016, "A Review of Radiofrequency Ablation: Large Target Tissue Necrosis and Mathematical Modelling," *Phys. Med.*, **32**(8), pp. 961–971.
- [7] Manuchehrabadi, N., and Zhu, L., 2014, "Development of a Computational Simulation Tool to Design a Protocol for Treating Prostate Tumours Using Transurethral Laser Photothermal Therapy," *Int. J. Hyperthermia*, **30**(6), pp. 349–361.
- [8] Chiang, J., Birla, S., Bedoya, M., Jones, D., Subbiah, J., and Brace, C. L., 2014, "Modeling and Validation of Microwave Ablations With Internal Vaporization," *IEEE Trans. Biomed. Eng.*, **62**(2), pp. 657–663.
- [9] ter Haar, G., and Coussios, C., 2007, "High Intensity Focused Ultrasound: Physical Principles and Devices," *Int. J. Hyperthermia*, **23**(2), pp. 89–104.
- [10] Jiang, C., Qin, Z., and Bischof, J., 2014, "Membrane-Targeting Approaches for Enhanced Cancer Cell Destruction With Irreversible Electroporation," *Ann. Biomed. Eng.*, **42**(1), pp. 193–204.
- [11] Jiang, C., Shao, Q., and Bischof, J., 2015, "Pulse Timing During Irreversible Electroporation Achieves Enhanced Destruction in a Hindlimb Model of Cancer," *Ann. Biomed. Eng.*, **43**(4), pp. 887–895.
- [12] Kingham, T. P., Karkar, A. M., D'Angelica, M. I., Allen, P. J., DeMatteo, R. P., Getrajdman, G. I., Sofocleous, C. T., Solomon, S. B., Jarnagin, W. R., and Fong, Y., 2012, "Ablation of Perivascular Hepatic Malignant Tumors With Irreversible Electroporation," *J. Am. Coll. Surg.*, **215**(3), pp. 379–387.
- [13] Thomson, K. R., Cheung, W., Ellis, S. J., Federman, D., Kavnoudias, H., Loader-Oliver, D., Roberts, S., Evans, P., Ball, C., and Haydon, A., 2011, "Investigation of the Safety of Irreversible Electroporation in Humans," *J. Vasc. Interv. Radiol.*, **22**(5), pp. 611–621.
- [14] Ben-David, E., Ahmed, M., Feroja, M., Moussa, M., Wandel, A., Sosna, J., Appelbaum, L., Nissenbaum, I., and Goldberg, S. N., 2013, "Irreversible Electroporation: Treatment Effect Is Susceptible to Local Environment and Tissue Properties," *Radiology*, **269**(3), pp. 738–747.
- [15] Bonakdar, M., Latouche, E. L., Mahajan, R. L., and Davalos, R. V., 2015, "The Feasibility of a Smart Surgical Probe for Verification of IRE Treatments Using Electrical Impedance Spectroscopy," *IEEE Trans. Biomed. Eng.*, **62**(11), pp. 2674–2684.
- [16] Neal, R. E., II, Garcia, P. A., Robertson, J. L., and Davalos, R. V., 2012, "Experimental Characterization and Numerical Modeling of Tissue Electrical Conductivity During Pulsed Electric Fields for Irreversible Electroporation Treatment Planning," *IEEE Trans. Biomed. Eng.*, **59**(4), pp. 1076–1085.
- [17] Sano, M. B., Fan, R. E., Hwang, G. L., Sonn, G. A., and Xing, L., 2016, "Production of Spherical Ablations Using Nonthermal Irreversible Electroporation: A Laboratory Investigation Using a Single Electrode and Grounding Pad," *J. Vasc. Interv. Radiol.*, **27**(9), pp. 1432–1440.
- [18] Hjouj, M., and Rubinsky, B., 2010, "Magnetic Resonance Imaging Characteristics of Nonthermal Irreversible Electroporation in Vegetable Tissue," *J. Membr. Biol.*, **236**(1), pp. 137–146.
- [19] Yao, C., Lv, Y., Dong, S., Zhao, Y., and Liu, H., 2017, "Irreversible Electroporation Ablation Area Enhanced by Synergistic High- and Low-Voltage Pulses," *PloS One*, **12**(3), p. e0173181.
- [20] Miklovic, T., Latouche, E. L., DeWitt, M. R., Davalos, R. V., and Sano, M. B., 2017, "A Comprehensive Characterization of Parameters Affecting High-Frequency Irreversible Electroporation Lesions," *Ann. Biomed. Eng.*, epub.
- [21] Wandel, A., Ben-David, E., Ulusoy, B. S., Neal, R., Faruja, M., Nissenbaum, I., Gourovich, S., and Goldberg, S. N., 2016, "Optimizing Irreversible Electroporation Ablation With a Bipolar Electrode," *J. Vasc. Interv. Radiol.*, **27**(9), pp. 1441–1450.
- [22] Phillips, M., 2014, "The Effect of Small Intestine Heterogeneity on Irreversible Electroporation Treatment Planning," *ASME J. Biomech. Eng.*, **136**(9), p. 091009.
- [23] Silve, A., Brunet, A. G., Al-Sakere, B., Ivorra, A., and Mir, L., 2014, "Comparison of the Effects of the Repetition Rate Between Microsecond and Nanosecond Pulses: Electroporation-Induced Electro-Desensitization?," *Biochim. Biophys. Acta*, **1840**(7), pp. 2139–2151.
- [24] Feroja, M., Ahmed, M., Appelbaum, L., Ben-David, E., Moussa, M., Sosna, J., Nissenbaum, I., and Goldberg, S. N., 2013, "Irreversible Electroporation Ablation: Is All the Damage Nonthermal?," *Radiology*, **266**(2), pp. 462–470.
- [25] Teissie, J., Golzio, M., and Rols, M., 2005, "Mechanisms of Cell Membrane Electroporation: A Minireview of Our Present (Lack of?) Knowledge," *Biochim. Biophys. Acta*, **1724**(3), pp. 270–280.
- [26] Ivorra, A., Al-Sakere, B., Rubinsky, B., and Mir, L. M., 2009, "In Vivo Electrical Conductivity Measurements During and after Tumor Electroporation: Conductivity Changes Reflect the Treatment Outcome," *Phys. Med. Biol.*, **54**(19), p. 5949.